

Supplementary Material

Ultrasound-mediated gene and drug delivery using a microbubble-liposome particle system

Young Il Yoon^{1,2,3*}, Yong-Su Kwon^{4*}, Hee-Sang Cho⁴, Sun-Hee Heo⁵, Kyeong Soon Park⁵, Sang Gyu Park⁵, Soo-Hong Lee⁵, Seung Il Hwang^{1,2}, Young Il Kim¹, Hwan Jun Jae¹, Gook-Jun Ahn⁷, Young-Seok Cho⁸, Hakho Lee⁹, Hak Jong Lee^{1,2,3,10}, Tae-Jong Yoon⁴

¹Department of Radiology, Seoul National University College of Medicine, Seoul 110-799, South Korea

²Department of Radiology, Seoul National University Bundang Hospital, Seungnam 463-707, South Korea

³Program in Nano Science and Technology, Department of Transdisciplinary Studies, Seoul National University Graduate School of Convergence Science and Technology, Suwon 443-270, South Korea

⁴Department of Applied Bioscience, College of Life Science, CHA University, Pocheon 135-081, South Korea

⁵Department of Biomedical Science, College of Life Science, CHA University, Pocheon 135-081, South Korea

⁶Department of Radiology, Seoul National University Hospital, College of Medicine, Seoul 110-744, South Korea

⁷Laboratory animal center, KBIO Osong Medical Innovation Foundation, Osong, Cheongwon, Chungbuk 363-951, South Korea

⁸Department of Gastroenterology, Uijeongbu St. Mary's Hospital, College of Medicine, The Catholic University of Korea, Uijeongbu 480-717, South Korea

⁹Center for Systems Biology, Massachusetts General Hospital, 185 Cambridge St, CPZN 5206, Boston, MA 02114, USA

¹⁰Nanoimaging and Therapy Research Center, Institute of Nanoconvergence, Advanced Institutes of Convergence Technology, Seoul National University

*These authors contributed equally to this work.

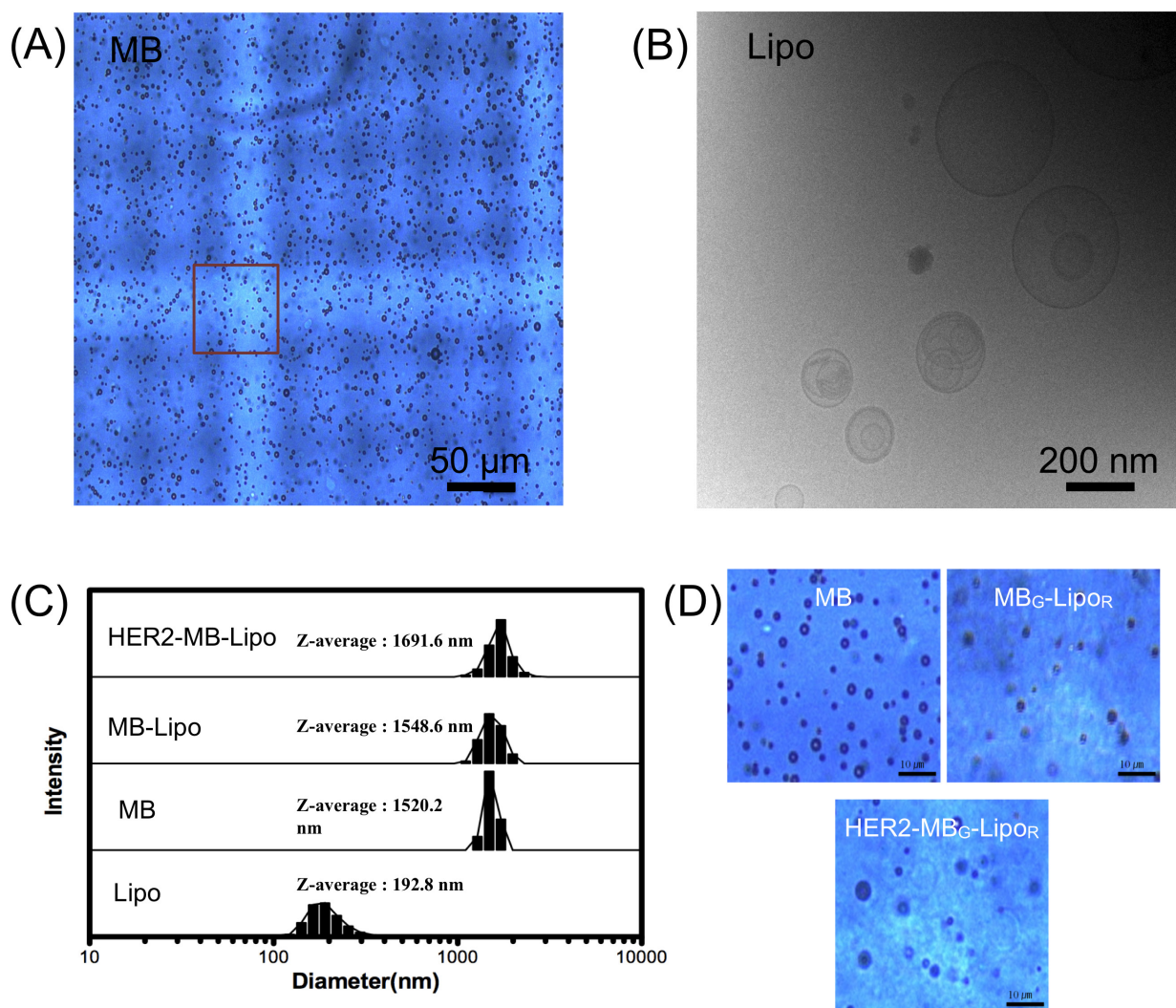


Fig. S1. Characterization for MB, Lipo and MB-Lipo complex particles. (A) Optical micrograph of MB particles. Individual particles are well dispersed. (B) Cryo electron micrograph of Lipo particles. (C) Dynamic light scattering analysis of MB, Lipos and MB-Lipo. The average sizes are 200 nm for Lipos and 1.5 μm for MBs. (D) Micrographs of MB, MB_G-Lipo_R and HER2-MB_G-Lipo_R. MBs maintained their shape and size after Lipo linking and antibody conjugation processes. Scale bar, 10 μm .

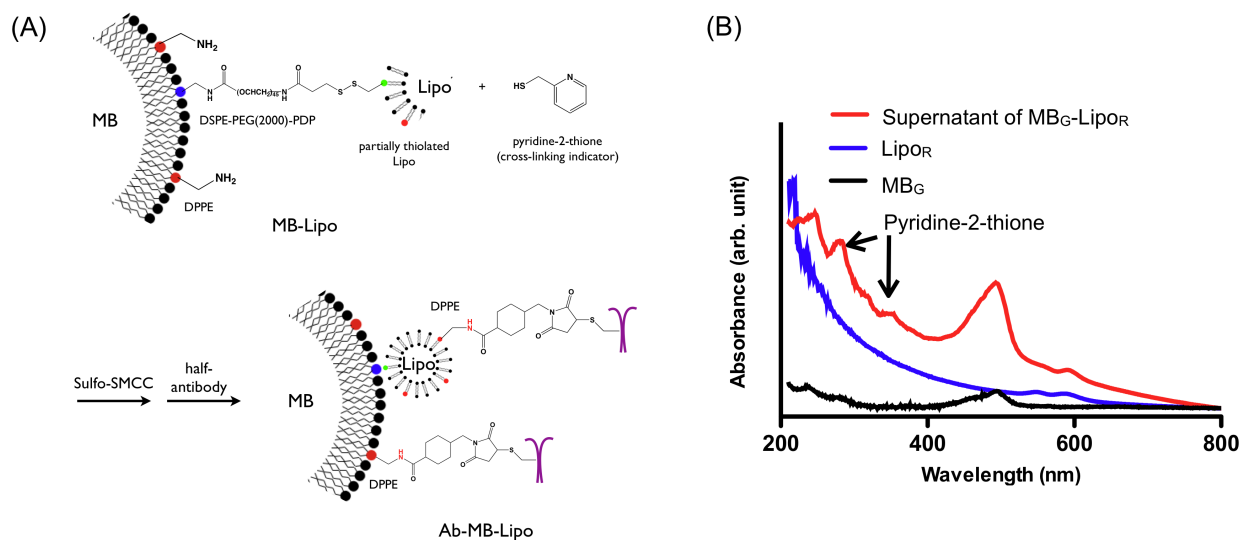


Fig. S2. MB-Lipo complex formation and antibody conjugation. (A) Surface modification chemistry. The DSPE-PEG(2000)-PDP lipid component of MBs was linked to thiol groups on the Lipo surface. Amines from DPPE on MB-Lipo complexes were reacted with amine-to-sulphydryl crosslinker (sulfo-SMCC), and further conjugated with half antibody. (B) After disulfide bond formation, pyridine-2-thione molecule was released from the DSPE-PEG(2000)-PDP, which can be detected by 2 peaks at 270 and 340 nm by UV-Vis spectroscopy.

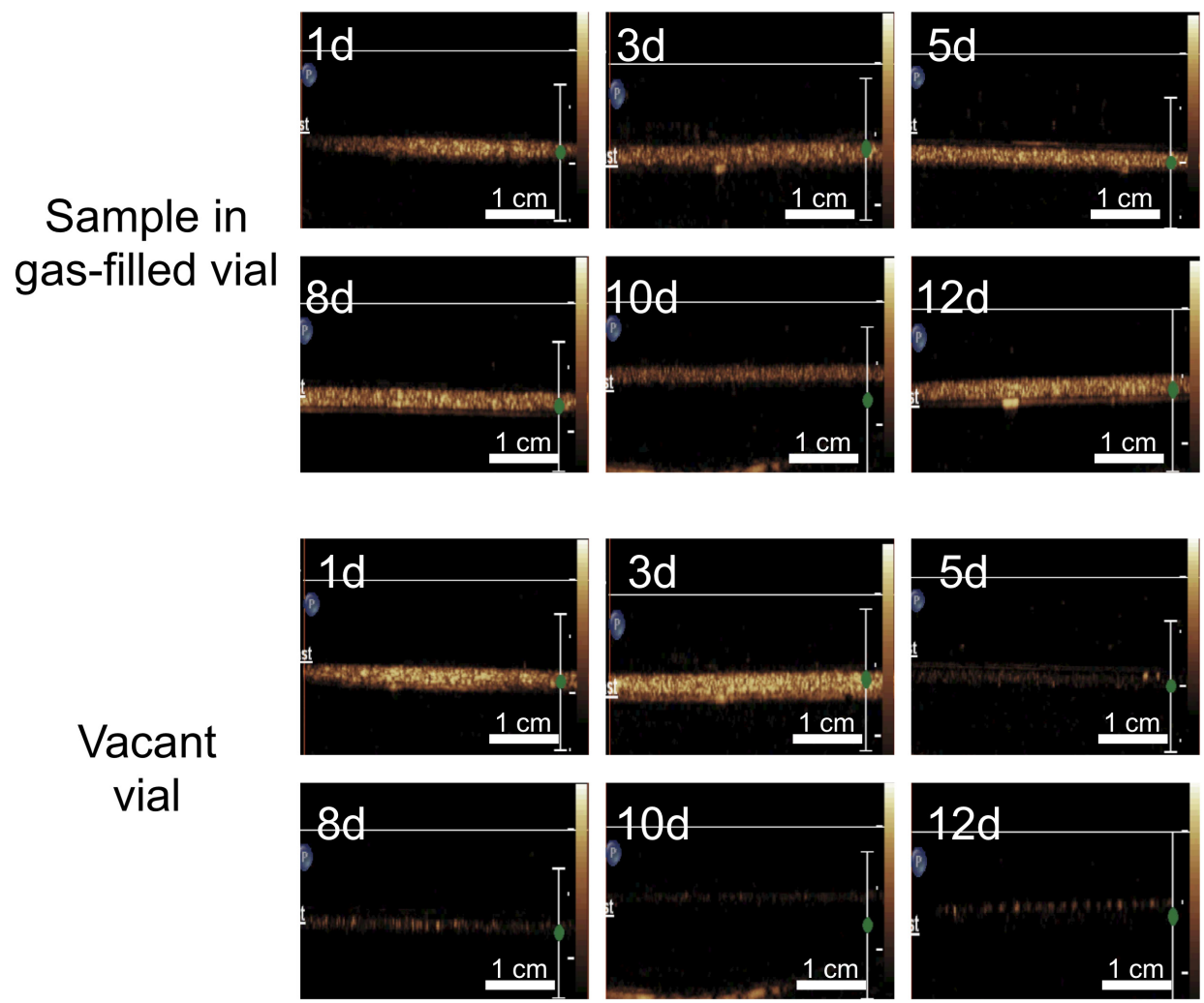


Fig. S3. Measurement for echogenicity stability during storage. Echogenicity and stability of the MB-Lipo particles were monitored. The MB-Lipo particles were stored in vials filled with SF₆ gas and demonstrated sustained signal intensity during a 2-week storage period, while samples in vacant vials showed decreasing intensity over time.

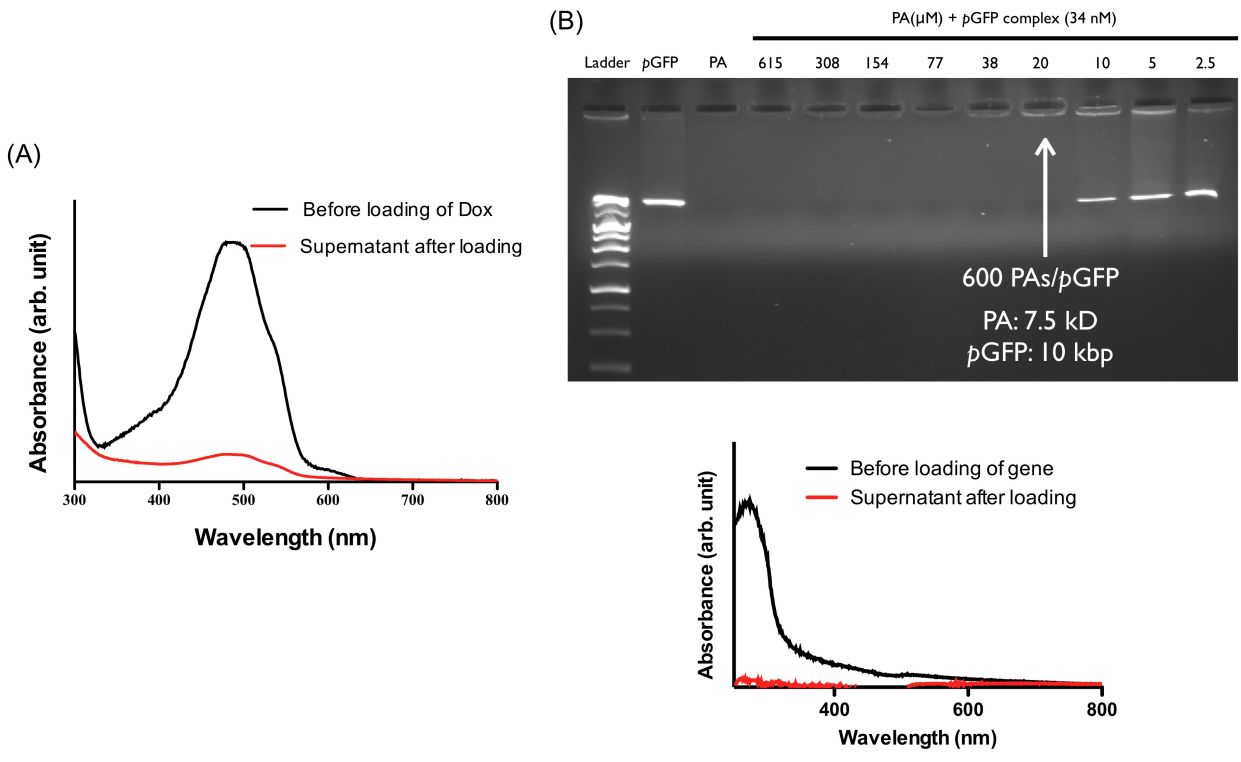


Fig. S4. Loading efficiency of drug and gene into the Lipo and optimization of PA and pGFP. Dox drug was easily encapsulated into the Lipo core through ammonium sulfate gradient method and determined the absorption spectrum by UV-Vis spectroscopy ($\lambda_{\text{max}} = 490 \text{ nm}$). It was decreased significantly the intensity of the supernatant after loading. The loading efficiency was calculated to 88.7 % into the Lipo (A). The molar ratio of complexed protamine (PA) and plasmid GFP (pGFP) was optimized, and the exact number of each molecule was characterized by electrophoresis (B, top). About 600 PAs (molecular weight of 7.5 kD) were linked with 1 pGFP (10 kbp). PA-pGFP complex solution was loaded into the Lipo_{Dox} particles after lyophilization, with a loading capacity of > 95 % effectiveness, as determined by UV-Vis absorption (B, bottom).

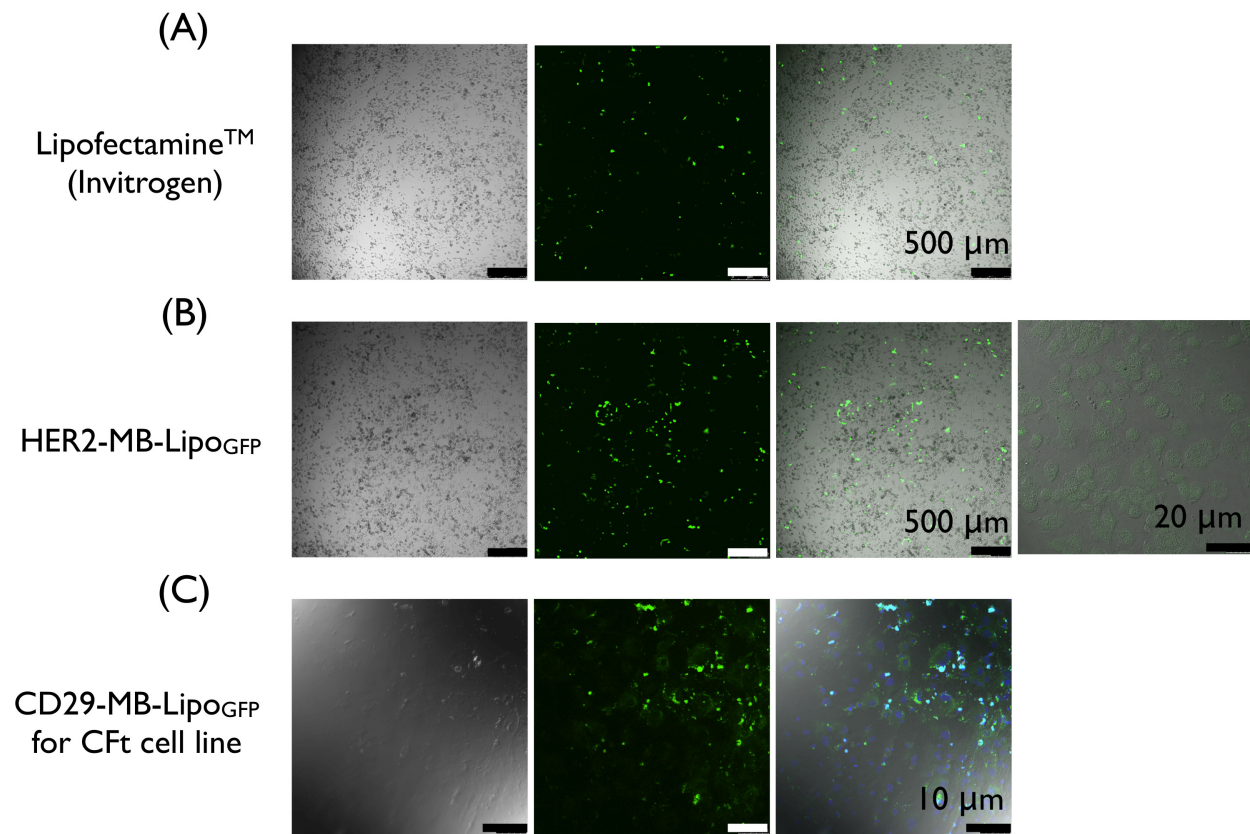


Fig. S5. Transfection efficiency for MB-Lipo particles. (A, B) Gene delivery efficiency of MB-Lipo particles was compared with that of a commercial transfection agent (Lipofectamine). GFP-expressing SkBr3 cells were observed as green dots. The MB-Lipo particle system was superior to deliver plasmid gene with > 300 % higher transfection efficiency, as compared to Lipofectamine. When visualized at a high magnification, most cancer cells had GFP expression in the cytoplasm (B, right). (C) The MB-Lipo particles were used to transfect primary cardiac fibroblast cells (CFt) with plasmid GFP gene. The transfection efficiency was ~ 60 %.

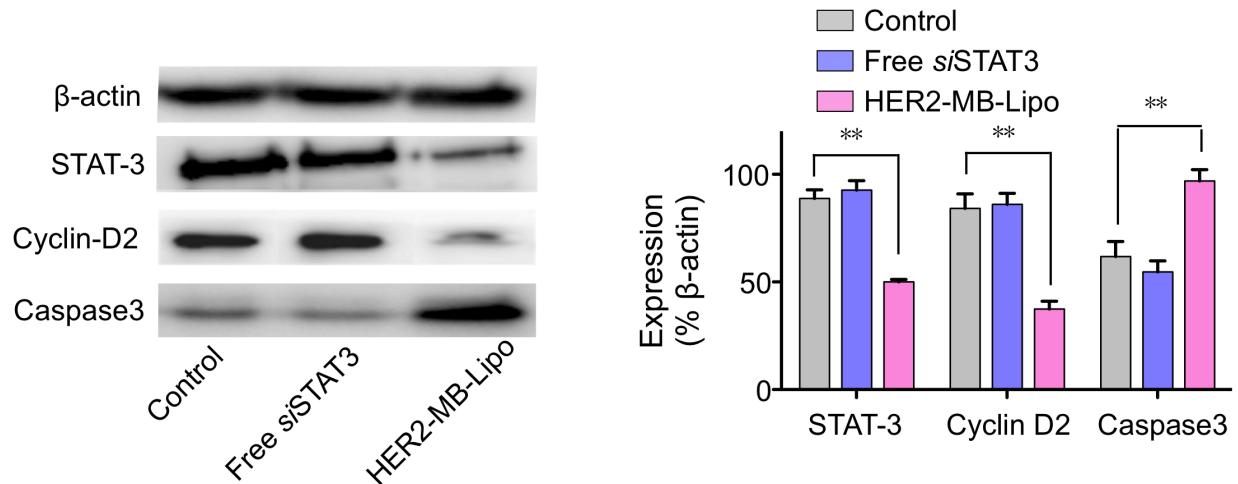
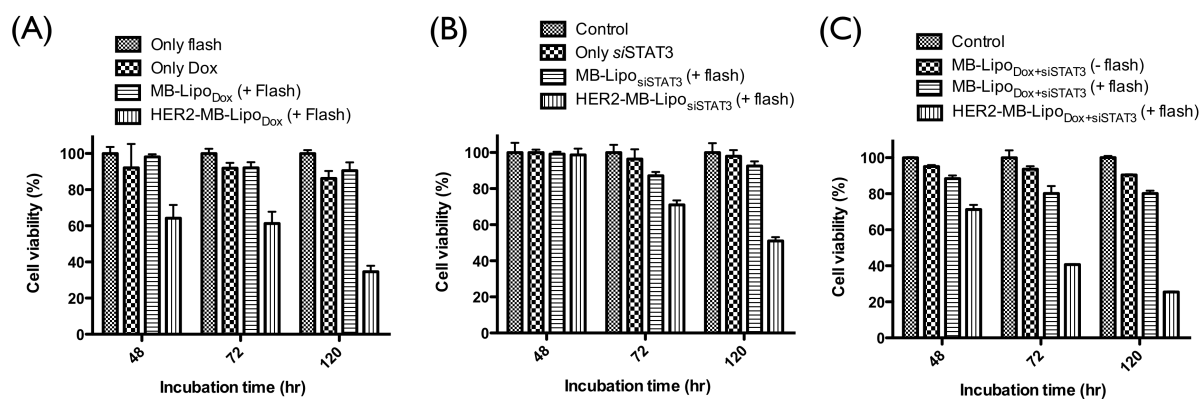


Fig. S6. Protein expression after treatment with MB-Lipo_{siSTAT3}. Cancer cells (SkBr3) were treated with HER2-MB-Lipo_{siSTAT3} and flash pulses, and their protein expression was analyzed by western blotting (left). The levels of STAT-3 and cyclin D2, related to cell proliferation, both decreased. On the other hand, the level of caspase3, an indicator of apoptosis, increased. Samples either non-treated or incubate with free siRNA showed negligible changes on these levels. All marker protein expressions were normalized with respective level of β -actin (right). Data are presented as the mean \pm SE from triplicate measurements. ** $p < 0.01$.



		Treatment	Cell viability (in 120 hr) mean \pm SD
Non-MB-Lipo	0.19 μ M Dox or 32 nM siSTAT3	Only flash	99.9 \pm 1.9
		Only Dox	86.2 \pm 4.1
		Only siSTAT3	97.9 \pm 3.4
MB-Lipo particle	Dox effect (0.19 μ M Dox)	MB-Lipo _{Dox} (+ flash)	90.5 \pm 4.5
		HER2-MB-Lipo _{Dox} (+ flash)	34.6 \pm 3.3
	siSTAT3 effect (32 nM siSTAT3)	MB-Lipo _{siSTAT3} (+ flash)	92.5 \pm 2.5
		HER2-MB-Lipo _{siSTAT3} (+ flash)	51.0 \pm 2.1
	Dox + siSTAT3 effect	MB-Lipo _{Dox+siSTAT3} (- flash)	90.4 \pm 0.4
		MB-Lipo _{Dox+siSTAT3} (+ flash)	80.1 \pm 1.6
HER2-MB-Lipo _{Dox+siSTAT3} (+ flash)		25.4 \pm 0.3	

Fig. S7. Therapeutic effect of MB-Lipo particles. Cell viability after treatment was determined using a typical cell proliferation assay (3-(4,5-Dimethylthiazol-2-yl)-2,5-Diphenyltetrazolium bromide, MTT). HER2-MB-LipoDox was determined a cell viability 34.6 % in 120 hr after treatment, but only Dox drug and non-antibody conjugated MB-Lipo_{Dox} were showed similar cell survival rate of > 85 % (A). And also, only siSTAT3, MB-Lipo_{siSTAT3}, or HER2-MB-Lipo_{siSTAT3} were revealed a cell viability of 97.9, 92.5 or 51 % (B). The treated cell sample with simultaneous Dox and siSTAT3 loaded HER2-MB-Lipo particle was the highest cell death of 25.4 % and non-antibody MB-Lipo particles possessing Dox and siSTAT3 were determined a cell viability of > 80 % (C). The cancer specific antibody conjugated particles were performed higher therapeutic effect than without antibody particles. And also, non-antibody MB-Lipo was not attached and introduced sonoporation/cavitation phenomenon around cell by flash treatment. Therefore, the treated cells with non-antibody MB-Lipo having drug or gene was revealed similar viability with only drug or gene treated cells. (All experiments in c and d were performed in triplicate. Data shows mean \pm SD).

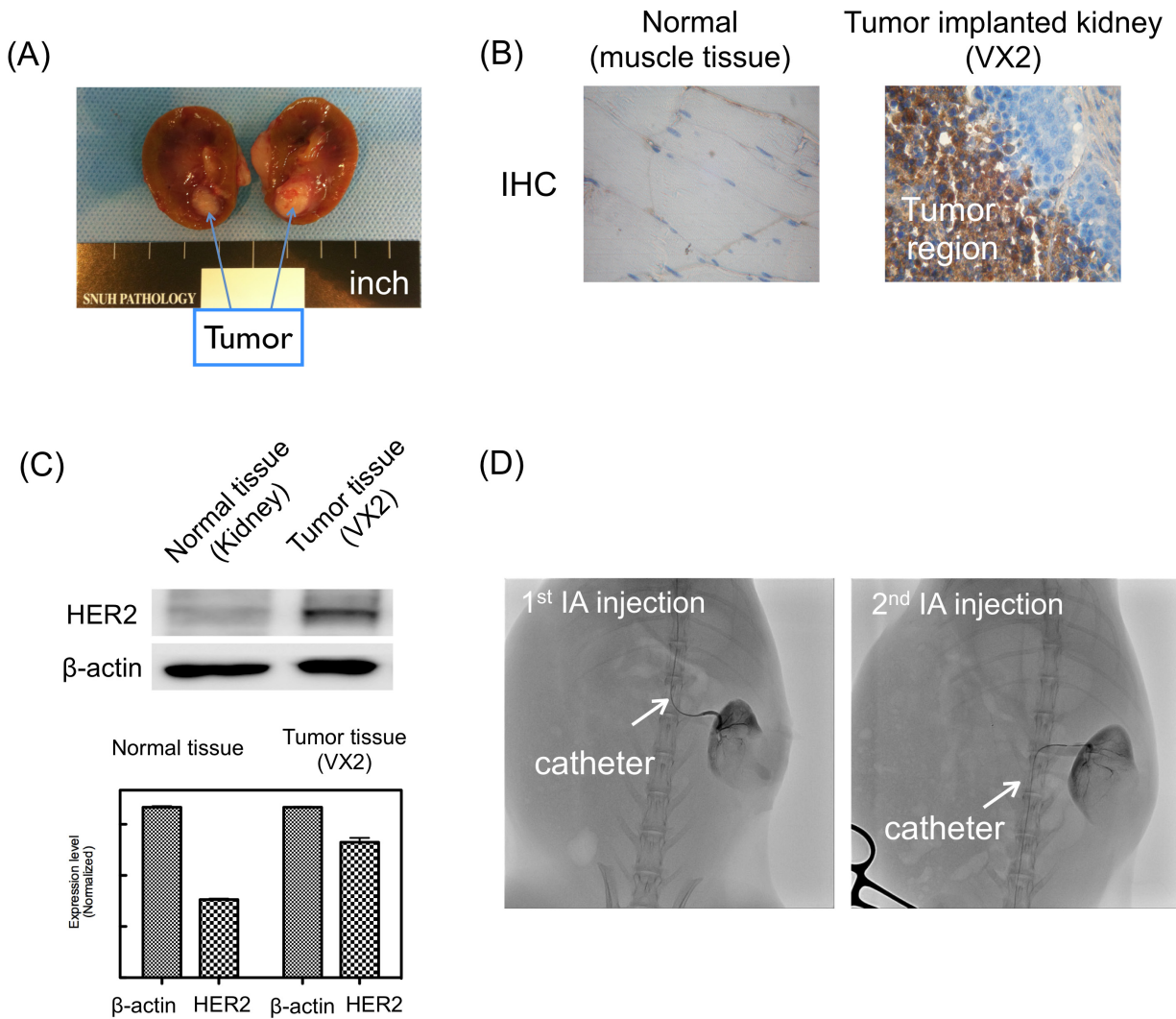


Fig. S8. VX2 tumor in kidney of a rabbit model and angiograph of IA injection of particles. (A) VX2 liver cancer cells were implanted in rabbit kidneys. (B) IHC staining was conducted in histological sections of embedded tumor (positive) and rabbit muscle tissues (negative control). The dark brown color representing EGFR expression was observed in the tumor region. (C) EGFR over-expression in the tumor site was further confirmed by western blotting. (D) Intra-arterial (IA) injection of the HER2-MB-Lipo_{Dox+siSTAT3} was performed using a catheter placed in the left renal artery of a rabbit (angiography images).

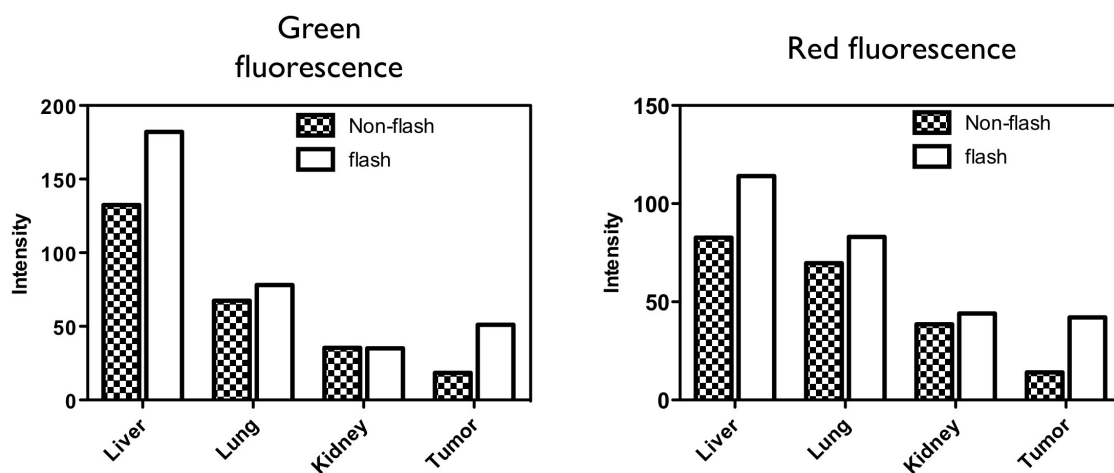
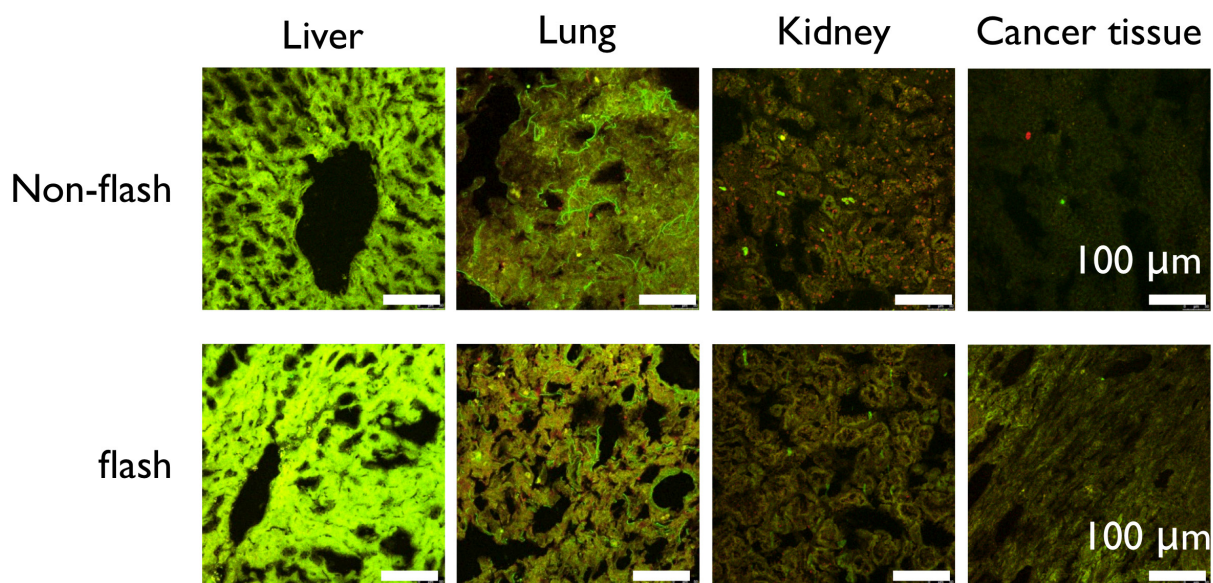


Fig. S9. Bio-distribution of MB-Lipo particles. The biodistribution of the fluorescent HER2-MB_G-Lipo_R particles was determined following intra-arterial (IA) injection. The organic dyes released from MB-Lipo by flash treatment were found in the liver, lungs, and kidneys as well as in the implanted tumors. Fluorescence intensity was the highest in the liver and lungs. In particular, the tumor tissue after flash exhibited higher green and red fluorescence intensities than tumors not exposed to flash.